Microporous Carbon Materials Derived From Sucrose as Sulfur Host for Lithium Sulfur Batteries

Yiqi Wang, Shuangke Liu*, Xiaobin Hong, Danqin Wang, Shiqiang Luo

College of Aerospace Science and Engineering, National University of Defense Technology, Changsha 410000, China

*Corresponding author e-mail: liu_sk@139.com

Abstract. Lithium sulfur batteries have attracted increasing attention due to its high theoretical specific capacity (1675 mAh g^{-1}) and high energy density (2600Wh kg^{-1}). However, to achieve the commercial application of lithium sulfur batteries, a cathode with excellent electrochemical performance is needed. Herein, we synthesized microporous carbon materials as sulfur host via a simple activation carbonization method. The MC/S delivered an excellent electrochemical performance. At 1 C rate, MC/S showed an initial discharge capacity of 899.5 mAh g^{-1}, and maintained a capacity of 617.6 mAh g^{-1} after 150 cycles corresponding to a capacity decay rate of 0.208% per-cycle.

1. Introduction

Lithium sulfur batteries have attracted increasing attention due to its high theoretical specific capacity and high energy density [1]. To overcome the issues of lithium sulfur batteries, such as "the shuttle effect", volume expansion during charge/discharge process and the low conductivity of cathode, researchers have done a lot of works [2, 3]. Porous carbon materials are wildly used as sulfur host due to its diverse advantages [4, 5]. Herein we used sucrose, a biomass sucrose, environment friendly, accessible and low cost material, as carbon sources and $FeCl_3$ as activator to synthesize microporous carbon (MC), and used it as sulfur host for lithium sulfur batteries. In contrast, we also synthesized sucrose derived bulk carbon (BC) which was not activated by $FeCl_3$ during carbonization process.

2. Experimental Section

2.1. Synthesis of MC and BC

1 g sucrose and 10 g $FeCl_3$ were dissolved in 60 ml ethanol aqueous solution (DI water: ethanol = 1:1 by volume). Then 0.1 M HCl was added drop-wise until pH=1. The solution was then evaporated at 100 °C under magnetic stirring. The obtained solid mixture was annealed at 900 °C for 2h (with a heating rate of 5 °C min^{-1} to 900 °C) under H_2/Ar (200 sccm/ 800 sccm). The carbonized product was soaked in 20 wt. % HCl solution for 24h. After washed by DI water and vacuum dried under 60 °C, MC was obtained. For comparison, BC was synthesized in the same procedure without $FeCl_3$.

2.2. Synthesis of MC/S and BC/S

MC/S was fabricated via a melting diffusion method. 0.1g MC and 0.4g sulfur was uniformly mixed. The mixture was heated at 155 ^{o}C under N_2 atmosphere for 8h to obtain MC/S composite. BC/S was obtained with the same procedure process.

2.3. Preparation of MC/S and BC/S cathode

80 wt. % MC/S, 12 wt. % super P carbon and 8 wt. % LA133 water soluble binder were mixed under magnetic string for 8h. The slurry was then coated on Al foil. After dried at 55^{o}C. The Vacuum dried cathode had a sulfur loading of 1.4-1.6 mg cm^{-2}.

2.4. Preparation of Li-S batteries

Lithium metal was used as anode. 1,3-dioxolane and 1,2-dimethoxyethane (DOL/DME, 1:1 by volume) with 0.5 M lithium bis-triuoromethanesulfonylimide (LiTFSI) and 0.4 M $LiNO_3$ was used as electrolyte. Celgard 2400 was used as separator. 16 uL per milligram of s electrolyte was added in cells. 2016 type coin-cells were used.

3. Results and Discussion

The micro-morphology of the synthesized MC and BC was shown in Figure 1. As shown in Figure 1a, b, it is clear that the particle size of BC range from 10 um to hundreds um. Besides, a smooth surface of BC is observed in Figure 1b. The morphology of MC is shown in Figure 1c, d. The particle size of MC is smaller than BC, indicating the activation of $FeCl_3$ could decrease the carbon particle size. Additionally, numerous pores are observed in Figure 1d which may be related to the activation of $FeCl_3$ [6]. The phenomenon demonstrated that $FeCl_3$ can promote the formation of porous structure.

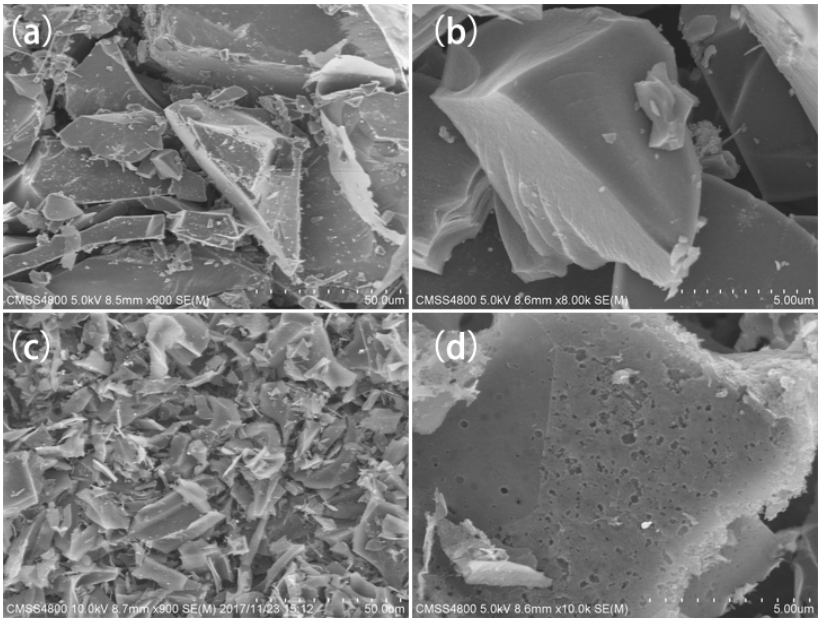

Figure 1. SEM images of BC (a, b), MC (c, d)

Normally, carbon materials derived from biomass materials show a low specific surface area and poor pore volume according to reported literatures [7, 8]. To investigate the detail of pores structure of MC, Brunauer–Emmett–Teller calculation was performed. The nitrogen adsorption/desorption isotherm of MC is type IV which indicates the existence of mesopores [9]. MC shows an ultrahigh surface area of 1853 m^2 g^{-1}. Moreover, the pore volume of MC is 0.999 cm^3 g^{-1}, and the micropore volume is 0.767 cm^3 g^{-1}. It is found that the majority of pores in MC is micropores, indicating $FeCl_3$

could facilitate the formation of micropores. The activation mechanism of $FeCl_3$ may be that $FeCl_3$ can promotes the degradation of sucrose and reacts with carbon forming meso/micropores [10].

To investigate the sulfur content of BC/S and MC/S, thermogravimetry analysis was used.As shown in figure 2b. The curve of MC/S showed two decrease plateaus. The first one corresponds to the evaporation of bulk sulfur or those restored in macropores or mesopores. The second one corresponds to the evaporation of sulfur confined in micropores due to the strong absorption force between sulfur particles and micropores [11]. It is noted that MC/S shows a sulfur content of 79.6 % whereas BC/S consists 75.1 % sulfur. The higher sulfur content of MC/S may be attributed to the higher pore volume.

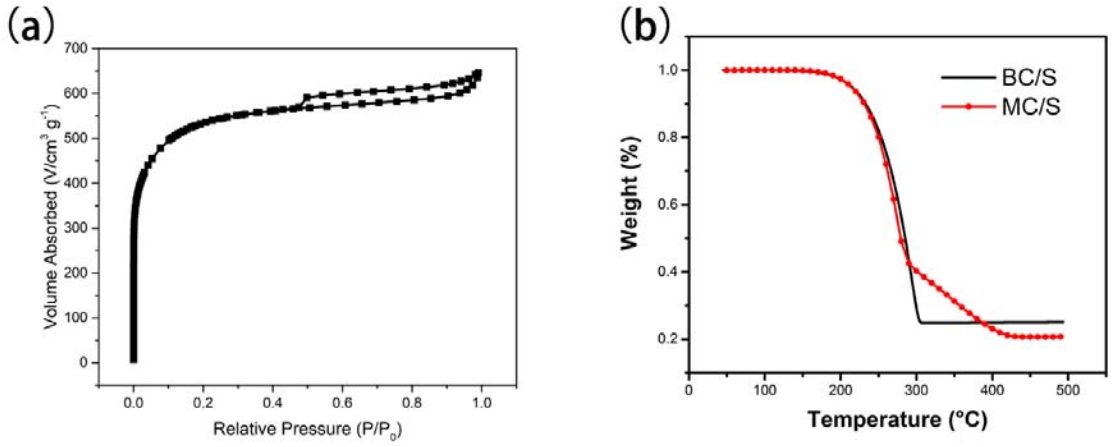

Figure 2. N_2 adsorption and desorption isotherms of MC and BC. (b) TGA curves of MC/S, BC/S and pure sulfur.

The charge/discharge curves of MC/S and BC/S were shown in Figure 3 (at 0.1C). The typical discharge curve of Li-S batteries usually show two plateaus. The first plateaus start at 2.3 V which indicates the transformation of S_8 to $S_{4\text{-}6}$. The second plateaus corresponded to the formation of Li_2S_2 and LiS_2 [12]. One charge plateaus is attributed to the transformation of Li_2S_2 and LiS_2 to S_8. As shown in Figure 3a, BC/S showed only one discharge plateaus during 1st cycle while a typical discharge plateaus at 15th cycle. Could decreases the potential of discharge plateaus [13]. As a result, the disappearance of the second plateaus maybe related to high polarization, caused by low electronic/ionic conductivity in BC/S. As can be seen in Figure 3b, MC/S showed two discharge plateaus at initial discharge indicating lower polarization. Compare to BC/S, the lower polarization of MC/S may be attributed to the porous structure which facilitates the infiltration of electrolyte and improved ionic conductivity [14].

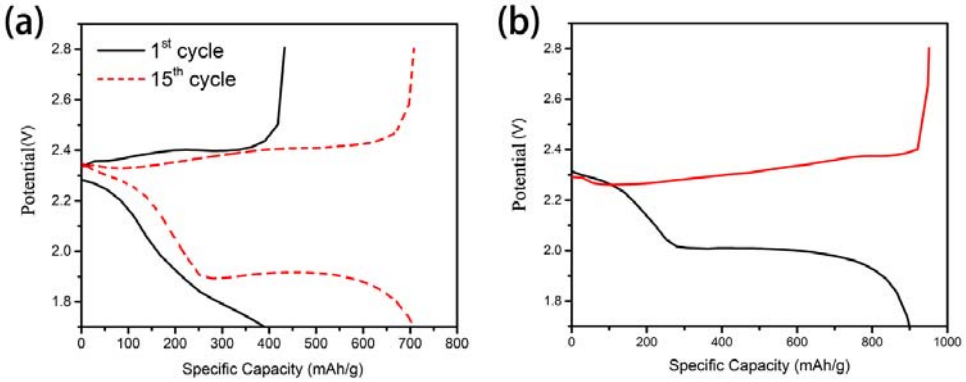

Figure 3. charge/discharge curves of MC/S (a), BC/S (b) at 0.1C.

To evaluate the long-term cycling performance, BC/S and MC/S were tested at 1 C. MC/S exhibited an initial discharge capacity of 899.5 mAh g^{-1}, and maintained a capacity of 617.6 mAh g^{-1} after 150 cycles corresponding to a capacity decay rate of 0.208% per cycle. BC/S showed a low initial discharge capacity of 390.3 mAh g^{-1}, and after an activation process, While BC/S reached a capacity of 707 mAh $g^{-1}$and an obviously decreased and unstable coulombic efficiency. The more stable performance of MC/S than BC/S may be attributed to porous structure which not only improves electronic/ionic conductivity but also restrains the loss of active sulfur [14, 15]. This phenomenon demonstrates that porous structure could improve the cycling stability and electrochemical reversibility.

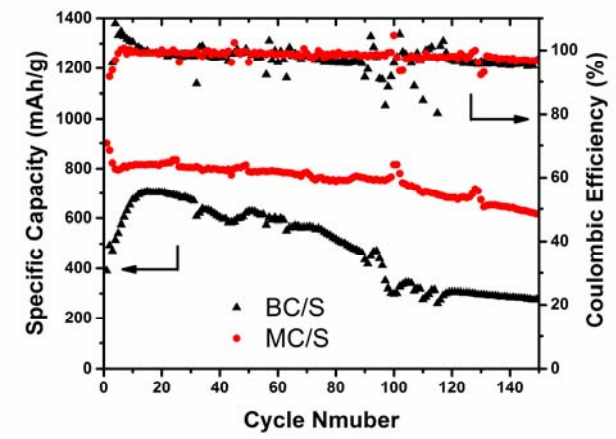

Figure 4. Long-term cycling performance of MC/S and BC/S at 1C

4. Conclusion

We synthesized microporous carbon materials as sulfur host via a simple activation carbonization. This method is facile, scalable and low cost which is suitable for industrialization. The as prepared MC showed a high surface area of 1853 m^2 g^{-1} and a pore volume of 0.999 cm^3 g^{-1}. With the porous structure, MC/S delivered a stable electrochemical performance. At 1C rate, MC/S showed a low capacity decay rate of 0.208% per cycle. This work offers an environmental friendly method to synthesize microporous carbon framework as sulfur host for lithium sulfur batteries.

Acknowlegments
We acknowledge the funding support of National Natural Science Foundation of China (No.51702362), and the National Postdoctoral Program for Innovative Talents (BX201700103).

References

[1] W. Kang, N. Deng, J. Ju, Q. Li, D. Wu, X. Ma, L. Li, M. Naebe, B. Cheng. A review of recent developments in rechargeable lithium-sulfur batteries, J. Nanoscale. 8 (2016) 16541-16588.
[2] T. Cleaver, P. Kovacik, M. Marinescu, T. Zhang, G. Offer. Commercializing Lithium Sulfur Batteries: Are We Doing the Right Research?, J. Journal of the Electrochemical Society. 165 (2018) A6029-A6033.
[3] A.N. Arias, A.Y. Tesio, V. Flexer. Review-Non-Carbonaceous Materials as Cathodes for Lithium-Sulfur Batteries, J. Journal of the Electrochemical Society. 165 (2018) A6119-A6135.
[4] Y. Xu, Y. Wen, Y. Zhu, K. Gaskell, K.A. Cychosz, B. Eichhorn, K. Xu, C. Wang. Confined Sulfur in Microporous Carbon Renders Superior Cycling Stability in Li/S Batteries, J. Advanced Functional Materials. 25 (2015) 4312-4320.
[5] G. Li, J. Sun, W. Hou, S. Jiang, Y. Huang, J. Geng. Three-dimensional porous carbon composites containing high sulfur nanoparticle content for high-performance lithium-sulfur batteries, J. Nat Commun. 7 (2016) 10601.
[6] H.Y. Zhao, X.A. Lu, Y. Wang, B. Sun, X.H. Wu, H.F. Lu. Effects of additives on sucrose-derived activated carbon microspheres synthesized by hydrothermal carbonization, J. Journal of Materials Science. 52 (2017) 10787-10799.
[7] Y. Gong, D. Li, C. Luo, Q. Fu, C. Pan. Highly porous graphitic biomass carbon as advanced electrode materials for supercapacitors, J. Green Chemistry. 19 (2017) 4132-4140.
[8] J. Zhang, J. Xiang, Z. Dong, Y. Liu, Y. Wu, C. Xu, G. Du. Biomass derived activated carbon with 3D connected architecture for rechargeable lithium-sulfur batteries, J. Electrochimica Acta. 116 (2014) 146-151.
[9] Y. Oda, K. Fukuyama, K. Nishikawa, S. Namba, H. Yoshitake, T. Tatsumi. Mesocellular foam carbons: Aggregates of hollow carbon spheres with open and closed wall structures, J. Chemistry of Materials. 16 (2004) 3860-3866.
[10] B. Wang, L. Zeng, W. Huang, F.S. Melkonyan, W.C. Sheets, L. Chi, M.J. Bedzyk, T.J. Marks, A. Facchetti. Carbohydrate-Assisted Combustion Synthesis To Realize High-Performance Oxide Transistors, J. Journal of the American Chemical Society. 138 (2016) 7067-7074.
[11] S. Choudhury, B. Kruener, P. Massuti-Ballester, A. Tolosa, C. Prehal, I. Grobelsek, O. Paris, L. Borchardt, V. Presser. Microporous novolac-derived carbon beads/sulfur hybrid cathode for lithium-sulfur batteries, J. J. Power Sources. 357 (2017) 198-208.
[12] X.Y. Liu, W.L. Huang, D.D. Wang, J.H. Tian, Z.Q. Shan. A nitrogen-doped 3D hierarchical carbon/sulfur composite for advanced lithium sulfur batteries, J. J. Power Sources. 355 (2017) 211-218.
[13] Y. Zhao, R. Tan, J. Yang, K. Wang, R.T. Gao, D. Liu, Y.D. Liu, J.L. Yang, F. Pan. 3D-hybrid material design with electron/lithium-ion dual-conductivity for high-performance Li-sulfur batteries, J. J. Power Sources. 340 (2017) 160-166.
[14] Y.-Z. Zhang, Z. Zhang, S. Liu, G.-R. Li, X.-P. Gao. Free-Standing Porous Carbon Nanofiber/Carbon Nanotube Film as Sulfur Immobilizer with High Areal Capacity for Lithium-Sulfur Battery, J. ACS applied materials & interfaces. (2018).
[15] W. Yang, W. Yang, A. Song, G. Sun, G. Shao. 3D interconnected porous carbon nanosheets/carbon nanotubes as a polysulfide reservoir for high performance lithium-sulfur batteries, J. Nanoscale. 10 (2018) 816-824.